

## Ultrafast spectroscopic studies of photoinduced electron transfer from semiconducting polymers to C<sub>60</sub>

B. Kraabel, D. McBranch,\* N. S. Sariciftci, D. Moses, and A. J. Heeger

*Institute for Polymers and Organic Solids, University of California at Santa Barbara, Santa Barbara, California 93106*

(Received 13 July 1994)

Using femtosecond time-resolved photoinduced absorption spectroscopy, we have studied the dynamics of photoinduced electron transfer from semiconducting polymers to C<sub>60</sub>. We find that with C<sub>60</sub> in poly[2-methoxy-5-(2'-ethyl-hexyloxy)-*p*-phenylene vinylene], poly(2,5-bis(cholestanoxo)-1,4-phenylene vinylene), and poly(3-octylthiophene) (P3OT), ultrafast photoinduced electron transfer occurs from the  $\pi^*$  band of the semiconducting polymer to the lowest unoccupied molecular-orbital level of C<sub>60</sub>. Time-resolved measurements of the dichroic ratio place a 300-fs upper limit on the electron transfer time. The charge-separated state is rendered metastable due to the spatial separation of the electron and hole and to polaron formation associated with the electron on the C<sub>60</sub> and the hole on the semiconducting polymer. Increasing the C<sub>60</sub> concentration in P3OT increases the lifetime of the charge-separated state. The two *p*-phenylene vinylene derivatives also displayed metastable charge separation.

### INTRODUCTION

The discovery of photoinduced electron transfer from a conducting polymer onto C<sub>60</sub> has been reported.<sup>1</sup> Photoinduced electron-spin-resonance experiments have clearly identified the spin-resonance signals of the polymer cation and C<sub>60</sub> anion.<sup>1</sup> The electron transfer quenches the luminescence in poly[2-methoxy-5-(2'-ethyl-hexyloxy)-*p*-phenylene vinylene] (MEH-PPV) by a factor of 10<sup>3</sup>, implying an electron-transfer time of less than one picosecond. Near steady-state photoinduced absorption (PIA) studies have demonstrated an excited-state absorption spectrum of the composite different from that of either the polymer or C<sub>60</sub> separately.<sup>2</sup> These observations stimulated a series of subpicosecond PIA experiments which directly measured the electron-transfer rate, confirming the estimate based on luminescence quenching.<sup>3</sup> The ultrafast electron transfer in the polymer/C<sub>60</sub> mixtures increases the quantum yield of *charged* photoexcitations on the polymer chain, resulting in an increase in the carrier lifetime and the magnitude of the photoconductivity.<sup>4</sup> This photoinduced electron transfer has been utilized to fabricate semiconducting polymer-C<sub>60</sub> heterojunction diodes, photodiodes, and solar cells.<sup>5</sup>

A number of factors influence the photoinduced charge transfer process. The ionization potential of the donor from the excited state ( $I_{D^*}$ ), the electron affinity of the acceptor ( $A_A$ ), and the Coulomb attraction of the separated radicals ( $U_C$ , which includes the dielectric or polarization screening of the separated charges), must satisfy the inequality

$$I_{D^*} - A_A - U_C < 0. \quad (1)$$

Even when this criterion is satisfied, the electron transfer can be inhibited by a faster competing processes, by a potential barrier preventing separation of the photoexcited

electron-hole pair, or by effects due to sample morphology which may prevent significant overlap of the donor and acceptor excited state wave functions.

The characterization of C<sub>60</sub> as an acceptor capable of accepting as many as six electrons<sup>6</sup> stimulated its use as an acceptor with conducting polymers (which are known to be weak donors). The ionization potentials and electron affinities of several conjugated polymers satisfy Eq. (1). Moreover, the relevant parameters can also be adjusted through manipulation of the band gap and electronegativity by molecular design.<sup>7</sup>

We find that in poly(3-octylthiophene) (P3OT) and in two soluble *p*-phenylene vinylene (PPV) derivatives, MEH-PPV and poly(2,5-bis(cholestanoxo)-1,4-phenylene vinylene) (BCHA-PPV), ultrafast photoinduced electron transfer occurs from the  $\pi^*$  band of the conjugated polymer to C<sub>60</sub>. By measuring the dichroic ratio, we have put an upper limit of 300 fs on the charge-transfer time. In P3OT/C<sub>60</sub> (1% by weight), the quantum efficiency for generation of *charged* photoexcitations is increased by the ultrafast charge transfer, but the lifetime of the charge-separated state is similar to the lifetime of the photoexcitations in the pristine polymer. Increasing the C<sub>60</sub> concentration to 10% (by weight) results in an increase in the lifetime of the charge-separated state by over an order of magnitude. The MEH-PPV and BCHA-PPV show slightly different behavior. In BCHA-PPV/C<sub>60</sub> (1% by weight) the relaxation kinetics of the PIA are identical to those of the pristine material until 7 ps, when the decay becomes significantly slower. This is not the case in MEH-PPV/C<sub>60</sub>, where the decay of the PIA is slower than that of the pristine material after only 300 fs. The possible role played by the side groups on the phenylene units on the charge-transfer process is discussed.

### EXPERIMENT

A dispersion compensated, colliding pulse mode-locked laser was used to produce a 96-MHz train of 100-fs pulses

at 2.01 eV. These pulses were subsequently amplified in a seven pass bowtie amplifier<sup>8</sup> pumped at 1.1 kHz by a frequency doubled Nd:YLF laser. The active gain medium consisted of a 2-mm flowing dye cell containing SR640 dye dissolved in ethylene glycol. A dye jet containing malachite green dissolved in ethylene glycol was placed between the sixth and seventh pass to serve as a saturable absorber. The amplified pulses were recompressed using two passes through a double prism arrangement. Pulse widths of 90–100 fs were routinely obtained, assuming a  $\text{sech}^2$  pulse profile, with pulse energies typically 2–3  $\mu\text{J}$ .

A 50% beam splitter was used to separate the amplified pulse beam into two beams, one of which was used as the pump beam. The other beam, focused using a 10-cm radius spherical mirror into a 3-mm cell of flowing ethylene glycol, produced a white-light continuum covering the spectral range from 500 to 1100 nm. The temporal profile of the continuum pulse was measured by cross correlation with the pump pulse via two-photon absorption in a GaP crystal,<sup>9</sup> yielding typical pulse widths of 200 fs for the continuum pulse. This cross-correlation measurement also enabled us to determine the chirp on the continuum pulse. We found a linear chirp from 600 to 1100 nm with a group velocity dispersion  $\Phi'' = 400 \text{ fs}^2$ , which results in a delay in the arrival time of the higher frequencies at the rate of 0.12 eV/100 fs.

The pump beam was passed through an optical delay line, then focused to a 0.09-mm<sup>2</sup> spot on the sample. Typical pump pulse energies at the sample were measured to be 1.2  $\mu\text{J}$ . The continuum beam served as the probe beam and was focused to a 0.025-mm<sup>2</sup> spot on the sample at the center of the pump beam spot. Careful alignment of the optical delay line ensured that the spatial overlap of the pump and probe spots on the sample did not change due to translation of the optical delay line. The pump and probe pulses were polarized parallel to each other for all measurements except for the dichroism measurement in which a half-wave plate was used to rotate the polarization of the pump pulse by  $\pi/2$ .

A portion of the probe beam was split off before reaching the sample to serve as the reference beam. The probe and reference beams were focused onto two vertically separated regions of a charge-coupled device (CCD) array. The transmitted spectrum of the probe beam was accumulated during an exposure of the CCD array and normalized by the spectrum of the reference beam (accumulated during the same exposure). The differential transmission ( $-\Delta T/T$ ) was calculated by subtracting the normalized spectrum with the pump on from the normalized spectrum with the pump off, and dividing by the normalized spectrum with the pump off. The change in optical absorption,  $\Delta ad$ , was calculated from the differential transmission using  $-\Delta T/T = 1 - \exp(-\Delta ad)$ . Background spectra were taken by blocking the probe and reference beams and accumulating one spectrum with the pump on, and one with the pump off. Possible effects from luminescence, dark current, and scattered light were then removed by subtracting the background from the corresponding spectrum after each accumulation.

Pristine P3OT was obtained from Neste Oy with a

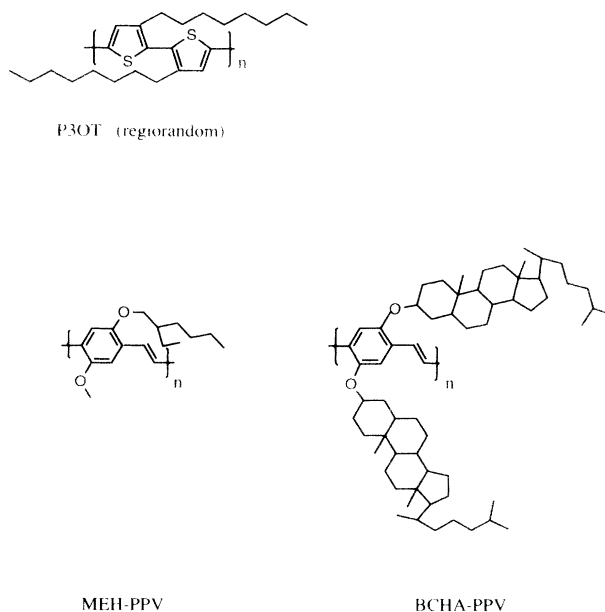


FIG. 1. Molecular structure of the polymers used in this study.

mean molecular weight of  $M_{av} \approx 9.6 \times 10^5$  and carefully purified and fractionated as previously described.<sup>2</sup> MEH-PPV and BCHA-PPV were obtained from UNIAX Corporation and used as received. Both PPV derivatives had  $M_{av} > 8 \times 10^6$  as determined by gel permeation chromatography relative to polystyrene as a standard. The chemical structure of the polymers used in this study are shown in Fig. 1. The polymer and polymer- $C_{60}$  samples were made in an argon atmosphere by dissolving the polymer and, when appropriate, a given percent by weight of  $C_{60}$ , in toluene or xylene, drop casting onto sapphire substrates, then evaporating off the solvent. The samples with low  $C_{60}$  concentration ( $< 10\%$ ) were homogeneous, while those with higher  $C_{60}$  content were nonuniform. All ratios of  $C_{60}$  to polymer refer to the ratio by weight. The samples were mounted onto the cold finger of a Heli-Tran system which allowed control of the temperature between 300 and 21 K. All samples were kept under vacuum while not in use; the experiments were carried out under a dynamic vacuum of  $10^{-5}$  torr.

## RESULTS AND DISCUSSION

### MEH-PPV, BCHA-PPV

The linear absorption spectra of MEH-PPV or BCHA-PPV show almost no change upon adding 1%  $C_{60}$  by weight.<sup>2</sup> For BCHA-PPV/ $C_{60}$  (1%), the optical-absorption band does not change at all upon addition of 1%  $C_{60}$ . In MEH-PPV/ $C_{60}$  a slight increase in the absorption is observed just below the band edge, probably due to disorder-induced band tailing. These results indicate that no significant overlap of the ground-state wave functions occurs, and hence that no charge transfer occurs in the ground state.

In the photoexcited state however, it has been demonstrated that electron transfer from MEH-PPV to  $C_{60}$  does occur.<sup>1,2</sup> From luminescence quenching the electron transfer was estimated to take place on the picosecond time scale. Subsequently, femtosecond PIA measurements demonstrated that charge transfer in P3OT/ $C_{60}$  actually occurred on the subpicosecond time scale.<sup>3</sup> Interpretation of the PIA spectra in the subpicosecond time regime is complicated by the chirp on the probe pulse. By measuring the dichroic ratio (to be discussed in more detail below) the time resolution is improved since we detect only a 100-meV band of the probe pulse at a given energy.

The photoinduced dichroism shown in Fig. 2 sets an upper limit on the time scale of the charge transfer. The dichroic ratio is defined as the ratio of the photoinduced absorption with the pump and probe polarization vectors parallel, to that with the polarization vectors perpendicular<sup>10</sup>

$$\frac{\Delta\alpha_{\parallel}}{\Delta\alpha_{\perp}} = \frac{3(f_e + f_{p_{\parallel}})\alpha_{\parallel} + f_{p_{\perp}}\alpha_{\perp}}{(f_e + f_{p_{\parallel}})\alpha_{\parallel} + 3f_{p_{\perp}}\alpha_{\perp}}. \quad (2)$$

In this expression the subscripts  $p_{\parallel}$  and  $p_{\perp}$  refer to intrachain and interchain excitations, respectively, and  $f_i$  is defined by  $f_i \equiv \eta_i \Delta\alpha_i(\omega)$ , where  $\eta_i$  is the quantum efficiency for generating excitations of type  $i$ , and  $\Delta\alpha_i(\omega)$  is the change in absorption due to these excitations. Because of the strong delocalization of the  $\pi$  electrons on an individual chain and the weak interchain coupling, the optical-absorption matrix elements are strongest when the light is polarized along the chains. Highly oriented MEH-PPV, for example, show  $\alpha_{\parallel}/\alpha_{\perp} \approx 100$ .<sup>11</sup> Thus, since the initially excited electron-hole pairs should be predominantly on individual chains, the dichroic ratio should be 3 at the earliest times. In the pure material the dichroic ratio will approach the isotropic value,  $\Delta\alpha_{\parallel}/\Delta\alpha_{\perp} = 1$ , after sufficient time has elapsed for interchain transfer or diffusion of the carriers over relatively long distances. If charge transfer from the polymer to  $C_{60}$  is more rapid, the charge-transfer process will quickly destroy any memory of the direction of the original transition dipole; hence, the dichroic ratio will approach the isotropic value more rapidly.

Measurements of the time decay of the dichroic ratio in MEH-PPV and BCHA-PPV provide insight into the dynamics of photoexcitations. As shown in Fig. 2, the initial value is close to 3 in both polymers, confirming that intrachain excitations are photogenerated by the pump radiation.

For the pure materials, the decay of the dichroism occurs over a relatively long time scale, with  $\Delta\alpha_{\parallel}/\Delta\alpha_{\perp}$  dropping from 3 to 2 in approximately 10 ps. This decay of the dichroic ratio is considerably faster than the lifetime of the photoluminescence (several hundred picoseconds).<sup>12</sup> Thus, either the polaron exciton diffuses over relatively large distances, or the electron and hole polarons separate and move independently on different chains. Which of these two mechanisms dominates remains unclear. Picosecond photoconductivity measurements would aid in resolving this issue.

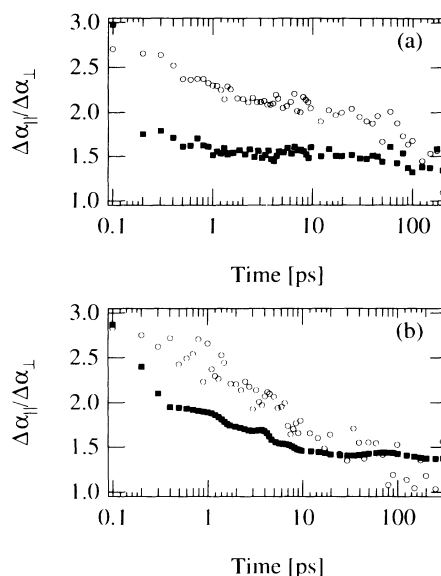


FIG. 2. (a) Dichroic ratio of MEH-PPV at 1.45 eV (open circles) and of MEH-PPV/ $C_{60}$  (1%) (closed squares) at 300 K. (b) Room-temperature dichroic ratio of BCHA-PPV at 1.45 eV (open circles) and of BCHA-PPV/ $C_{60}$  (1%) (closed squares).

In both MEH-PPV/ $C_{60}$  and BCHA-PPV/ $C_{60}$  the initial dichroic ratio at 1.45 eV is again close to 3. The addition of 1%  $C_{60}$ , however, causes  $\Delta\alpha_{\parallel}/\Delta\alpha_{\perp}$  to decay to less than 2 within a few hundred femtoseconds (Fig. 2). Since charge transfer will quickly destroy any memory of the direction of the original transition dipole, the rapid decrease in the dichroism is attributed to the ultrafast charge transfer. This measurement sets an upper limit of 300 fs on the photoinduced electron transfer time.

The dramatic change in dichroic ratio is too fast to be accounted for by diffusion of the photoexcitations over the distance necessary for losing the polarization memory. This time is at least on the order of 10 ps from the decay of the dichroic ratio in pristine MEH-PPV and BCHA-PPV. In addition, the sharp, nearly discontinuous change in the decay of the dichroism in the composites (see especially the MEH-PPV/ $C_{60}$  data in Fig. 2) after several hundred femtoseconds argues against diffusion of the excitations; loss of polarization memory by diffusion would yield a smooth decay, as seen in pristine MEH-PPV and BCHA-PPV. Thus we conclude that ultrafast photoinduced charge transfer destroys the polarization memory within 300 fs.

The PIA spectrum and its time evolution after photoexcitation are altered significantly upon addition of  $C_{60}$ , consistent with photoinduced electron transfer. The time-resolved PIA spectra are shown in Figs. 3 and 4; Figs. 3(a) and 4(a) show the spectra for the pure polymers and Figs. 3(b) and 4(b) show the data for the polymer- $C_{60}$  mixtures. For both BCHA-PPV/ $C_{60}$  (1%) and MEH-PPV/ $C_{60}$  (1%), a broad absorption band centered near 1.45 eV is observed in the PIA spectrum. In both cases the spectra are different from that observed in the pure polymer; i.e., without the  $C_{60}$ . In contrast to P3OT/ $C_{60}$

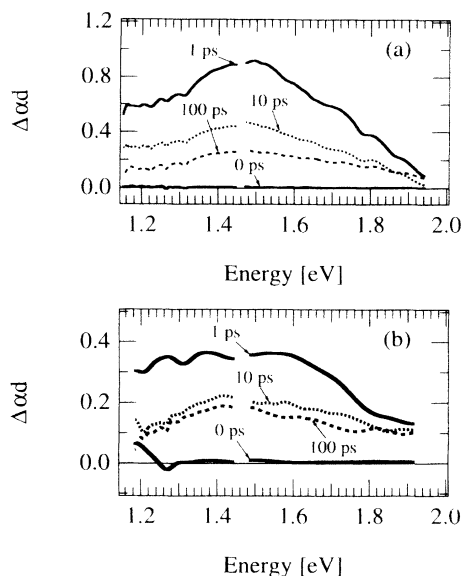


FIG. 3. Photoinduced absorption spectra at 300 K at various delay times after a 2.01-eV, 100-fs pump pulse in (a) MEH-PPV and (b) MEH-PPV/C<sub>60</sub> (1%).

(to be discussed in more detail below), the PIA band which characterizes the charge-transferred (CT) state forms at 1.45 eV, with no observable redshift as time evolves.

The PIA spectrum for MEH-PPV/C<sub>60</sub> (1%) [Fig. 3(b)] at 1 ps is very similar to the PIA spectrum observed in the ms time regime,<sup>2</sup> with a shoulder on the low-energy side of the peak, and a plateau above 1.8 eV. Light-induced electron spin resonance (LESR) experiments demonstrated that this spectral feature is associated with photoinduced electron transfer from MEH-PPV to

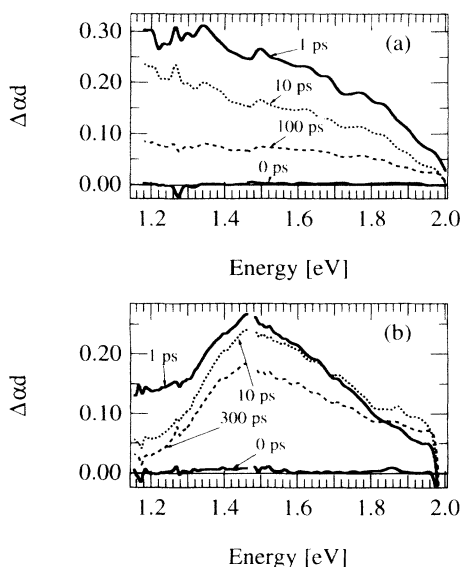


FIG. 4. Photoinduced absorption spectra at 300 K at various delay times after a 2.01-eV, 100-fs pump pulse for (a) BCHA-PPV and (b) BCHA-PPV/C<sub>60</sub> (1%).

C<sub>60</sub>.<sup>1,2</sup> Therefore, the observation of the same species at 1 ps that is observed in the ms time regime provides direct evidence that the photoinduced electron transfer occurs on a subpicosecond time scale, consistent with the results of the dichroic ratio measurement.

In BCHA-PPV/C<sub>60</sub> an absorption band peaking at 1.45 eV forms with a risetime that is resolution limited [see Fig. 4(b)]. The PIA spectra demonstrate that this band is clearly of a different origin than the PIA spectrum of pure BCHA-PPV [Fig. 4(a)]. Again, we assign the 1.45-eV PIA band in BCHA-PPV/C<sub>60</sub> (1%) to the charge-separated state, with the electron on C<sub>60</sub> and the hole on the polymer chain. The 1.45-eV PIA band is similar to that observed in MEH-PPV/C<sub>60</sub> and P3OT/C<sub>60</sub> (1%). Hence, the PIA spectrum is consistent with the conclusion that electron transfer in BCHA-PPV/C<sub>60</sub> occurs within several hundred femtoseconds of photoexcitation.

Once the electron and hole become spatially separated, the electron on C<sub>60</sub> may thermalize from the initial high-energy state to the *t*<sub>1u</sub> state and then to the negative polaron,<sup>13</sup> while the hole on the polymer chain will relax to form a positively charged polaron. This polaron formation certainly contributes to the relatively long lifetime of the CT state, as demonstrated by the decay of the PIA at 1.45 eV in the MEH- and BCHA-PPV/C<sub>60</sub> composites (Figs. 5 and 6).

We used the following function to fit the relaxation kinetics:<sup>14</sup>

$$\Delta\alpha(\tau) \propto \int dt I_{pb}(t-\tau) \int dt' \theta(t-t') R(t-t') I_{pp}(t'). \quad (3)$$

In this expression  $\tau$  is the relative time delay between the

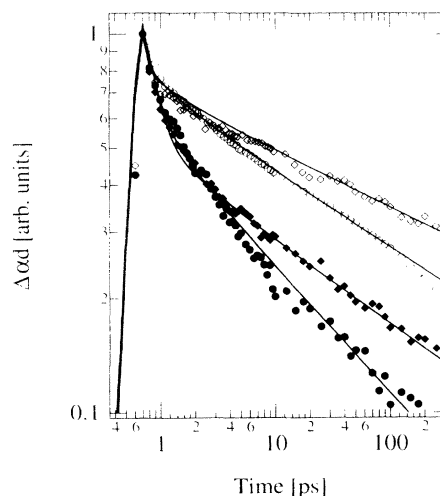


FIG. 5. The decay of the photoinduced absorption at 1.45 eV in MEH-PPV, at 300 K (closed circles), and at 86 K (closed diamonds), and at the same energy in MEH-PPV/C<sub>60</sub> (1%) at 300 K (open circles), and at 86 K (open diamonds). The fits are to  $R(t) = At^{-\alpha} + Be^{-t/\tau}$  with  $\tau=300$  fs and  $\alpha=0.33$  for pristine MEH-PPV at 300 K and  $\tau=300$  fs and  $\alpha=0.2$  at 86 K. For MEH-PPV/C<sub>60</sub>  $\tau=100$  fs and  $\alpha=0.2$  at 300 K and  $\tau=100$  fs and  $\alpha=0.15$  at 86 K.

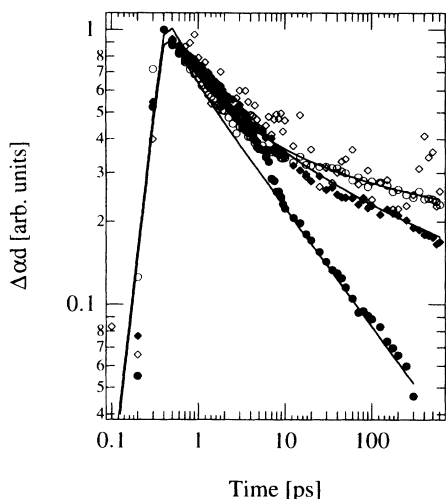


FIG. 6. Time decay of the photoinduced absorption at 1.45 eV in BCHA-PPV at 300 K (closed circles), and at 21 K (closed diamonds). Also shown are the dynamics of BCHA-PPV/C<sub>60</sub> (1%) at 1.45 eV, 300 K (open circles), and at 86 K (open diamonds). The fits are to  $R(t) = At^{-\alpha}$  with  $\alpha = 0.43$  for pristine BCHA-PPV at 300 K and to  $R(t) = At^{-\alpha_1} + Bt^{-\alpha_2}$  with  $\alpha_1 = 0.12$  and  $\alpha_2 = 0.6$  at 21 K. At 300 and 86 K in BCHA-PPV/C<sub>60</sub> (1%)  $\alpha_1 = 0.05$  and  $\alpha_2 = 0.6$ .

pump and the probe pulses, and  $I_{pp}$  represents the pump pulse intensity profile, which was measured using second harmonic generation in a KDP crystal. The fit to a sech<sup>2</sup> pulse shape yielded a 100-fs pulse width.  $I_{pb}$  represents the probe pulse intensity profile, which was obtained by deconvoluting the measured cross correlation of the probe and pump pulse.  $\theta(t-t')$  is a step function and  $R(t-t')$  is the response function which describes the dynamics of the system.

The decay of the PIA at 300 K in MEH-PPV is fit using the response function  $R(\tau) = Ae^{-\tau/\tau} + Bt^{-\alpha}$  with  $\tau = 300$  fs, and a slow power-law tail,  $t^{-0.33}$  (Fig. 5, closed circles). Upon cooling to 86 K, the fast component remains unchanged, but the longer-lived component decays more slowly,  $t^{-0.22}$  (solid diamonds). The data suggest the existence of an energy barrier that must be overcome in order for the electron and hole to recombine. Upon addition of 1% C<sub>60</sub>, the time constant of the fast exponential component decreases to 100 fs, and the power-law decay becomes much slower. At 300 K (open circles) the latter follows  $t^{-0.2}$ , which at 86 K (open diamonds) becomes  $t^{-0.15}$ . The decrease in the lifetime of the fast exponential is attributed to the influence of the ultrafast charge transfer. A charge transfer time of 150 fs in parallel with the 300-fs time constant of pristine MEH-PPV would yield the observed 100-fs time constant. This is consistent with the dichroic ratio data which show that the charge transfer occurs on the hundred femtosecond time scale.

After several hundred femtoseconds, however, the decay becomes much slower in the composite material than

in the pristine material, consistent with the known metastability of the charge-separated state. This observation is consistent with photoconductivity measurements which showed an increase in the magnitude and lifetime of the photocurrent upon addition of 1% C<sub>60</sub>.<sup>4</sup> The slight temperature dependence of the relaxation time ( $t^{-0.15}$  at 86 K versus  $t^{-0.2}$  at 300 K) is consistent with measurements of the temperature dependence of the LESR signal in MEH-PPV/C<sub>60</sub> (50%). An Arrhenius behavior was found for the back-transfer process (electron on C<sub>60</sub> transferring back to polymer) with an activation energy of 15 meV.<sup>2</sup> This energy barrier inhibits the recombination process and may account for the slower kinetics observed at lower temperatures. From our measurements, however, it is not clear whether the activation barrier inhibits the back-transfer rate (transfer of electron from C<sub>60</sub><sup>-</sup> to polymer) or whether it reduces the recombination rate of electrons and holes on the polymer chain (as is the case in pristine MEH-PPV) after the back-transfer process is completed.

The relaxation kinetics of BCHA-PPV/C<sub>60</sub> at 1.45 eV show a dramatic increase in lifetime over that of the pristine material. However, in this PPV derivative, the decay of the PIA does not become metastable until approximately 7 ps after photoexcitation (Fig. 6). The kinetics of the long-lived PIA at 1.45 eV in BCHA-PPV (closed circles) follows  $R_1(t) = At^{-0.43}$ , which can be interpreted in terms of geminate recombination of two excitations after executing a one-dimensional random walk.<sup>15,16</sup> At 21 K the response function is  $R_2(t) = At^{-\alpha_1} + Bt^{-\alpha_2}$ , with the fast component following  $t^{-0.6}$  and the slow component decaying as  $t^{-0.12}$ . The addition of 1% C<sub>60</sub> results in PIA dynamics which fit the same  $R_2(t)$  functional form as given above, with the same  $\alpha_1$  ( $=0.6$ ), but with  $\alpha_2 = 0.05$ . The slower decay in BCHA-PPV/C<sub>60</sub> results from charge separation and trapping of the electron on the C<sub>60</sub>. Unlike the dynamics in the pristine material, these kinetics are temperature independent between 300 and 21 K, supporting the conclusion that the relaxation pathway of the photoexcitations is different in the composite than in pristine BCHA-PPV.

The fact that the dynamics of the PIA in BCHA-PPV/C<sub>60</sub> are identical to that of the pristine polymer for the first 7 ps after photoexcitation is different from what we observe in MEH-PPV/C<sub>60</sub>, where the photoexcitations become metastable after only several hundred femtoseconds. The results of the dichroic ratio measurement of the two composites also show slightly different results for  $\tau < 7$  ps (Fig. 2). In BCHA-PPV/C<sub>60</sub> (1%) the dichroism drops from 2.8 to 1.8 in the first 300 fs, then slowly decays to below 1.5 within 7 ps, after which it stabilizes at approximately 1.4. The data for MEH-PPV/C<sub>60</sub> show the dichroism dropping from 3 to 1.75 in 100 fs, and then to 1.5 by 1 ps, where it remains constant over more than 100 ps. These results suggest that a larger fraction of the initial photoexcitations undergo ultrafast (within 300 fs) charge transfer in MEH-PPV/C<sub>60</sub> (1%) than in BCHA-PPV/C<sub>60</sub> (1%). The remaining photoexcitations that have not undergone charge transfer are presumably intrachain excitations as in the pristine poly-

mer, and would therefore account for the higher value of the dichroic ratio seen in this composite between 200 fs and 7 ps. The slow decay of the dichroic ratio between 200 fs and 7 ps may result from the diffusion of these photoexcitations, prior to charge transfer, to chain segments that are randomly oriented with respect to the initial chain segment.

Since 1% by weight corresponds to roughly 300 monomer units per  $C_{60}$  in MEH-PPV/ $C_{60}$  and 100 monomer units per  $C_{60}$  in BCHA-PPV/ $C_{60}$ , the diffusion time of the photoexcitations cannot account for the increased time it takes for all the photoexcitations to undergo charge transfer in BCHA-PPV/ $C_{60}$ , because the photoexcitations have to diffuse less far to reach a  $C_{60}$  molecule in this polymer than in MEH-PPV. In addition, the density of  $C_{60}$  in the polymer host exceeds the photoexcitation density used in this study, so that multiple electron transfer to a single  $C_{60}$  acceptor is not considered important for either PPV derivative.

Although currently no measurement of the ionization potential of BCHA-PPV has been reported, calculations indicate that the ionization potential of different PPV derivatives can differ by several hundred meV.<sup>17</sup> A difference in ionization potential between MEH-PPV and BCHA-PPV could influence the electron transfer rate. However, since the electron transfer rate in MEH-PPV/ $C_{60}$  and in P3OT/ $C_{60}$  (to be discussed below) are comparable in spite of the different ionization potentials of these two polymers, we do not consider this mechanism to be the main reason for the difference in the charge-transfer efficiency in the two PPV derivatives.<sup>18</sup> If the electron transfer occurred via an activation process, we would expect a temperature dependence on the electron transfer rate, contrary to our observation. Instead we suggest that this delay in achieving charge transfer of all photoexcitations in BCHA-PPV/ $C_{60}$  is due to the influence of the bulky, symmetric side groups of this polymer (Fig. 1), making it more difficult to achieve significant overlap of the excited-state wave function with a  $C_{60}$  molecule. This same mechanism may also inhibit the back-transfer process, accounting for the slower decay of the photoexcitations in BCHA-PPV/ $C_{60}$  after 7 ps than in MEH-PPV/ $C_{60}$  (compare  $t^{-0.15}$  in MEH-PPV/ $C_{60}$  to  $t^{-0.05}$  in BCHA-PPV/ $C_{60}$ ).

### P3OT

The time-resolved photoinduced absorption spectra of pristine P3OT and of P3OT with 1%  $C_{60}$  are shown in Figs. 7(a) and 7(b), respectively. The spectrum for the pristine material consists of two distinct features, one at 1.9 eV and one at 1.2 eV, which we shall refer to as the high-energy (HE) feature and the low-energy (LE) feature, respectively. After 10 ps there is no change in the relative spectral weight of the HE and LE features; the spectrum at 250 ps can be scaled to precisely fit the spectrum at 10 ps.

The time evolution of the HE feature consists of two components, a fast exponential component with a lifetime of 800 fs, and a slow component which matches the dynamics of the LE feature.<sup>19</sup> The fast component of the

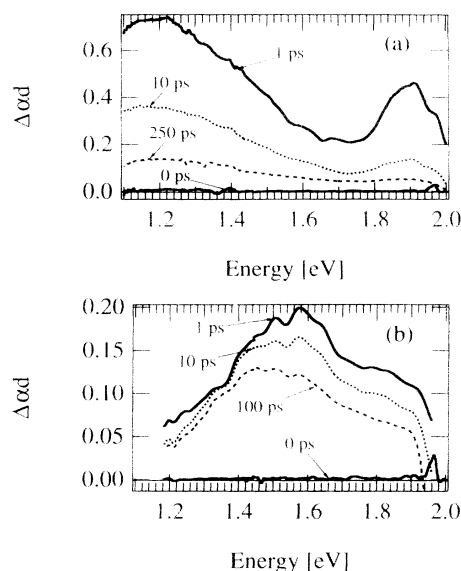


FIG. 7. Room-temperature photoinduced absorption spectra at various delay times after a 2.01-eV, 100-fs pump pulse in (a) P3OT and (b) P3OT/ $C_{60}$  (1%).

HE feature matches that seen in poly(3-methylthiophene)<sup>20</sup> and polythiophene,<sup>21</sup> and has been attributed to a self-trapped singlet exciton, or a singlet polaron exciton. A different photoexcitation gives rise to the dual bands (the LE feature and the long-lived component of the HE feature), with dynamics that follow a stretched exponential decay ( $Ae^{-(t/\tau)^\beta}$ , with  $\beta = \frac{1}{3}$ ). One possible origin of the stretched exponential decay is one-dimensional diffusion,<sup>22,23</sup> in which the excitations diffuse along the polymer chains among randomly distributed recombination centers. These two long-lived PIA bands originate from the same species: for  $\tau > 20$  ps, they display the same time dependence, intensity dependence, and temperature dependence, as well as the same dichroic ratio (discussed in more detail below).

Upon adding  $C_{60}$  to P3OT, the PIA spectrum, decay kinetics, and intensity dependence all change dramatically. At concentrations of 1% or more by weight, the linear absorption spectrum shows a broadening, and a slight blueshift, of the  $\pi$ - $\pi^*$  band with a tail extending into the gap. The spectrum is similar to that reported previously,<sup>2</sup> and is attributed to partial charge transfer in the ground state, from  $DA \rightarrow D^{\delta+} + A^{\delta-}$  (where  $D$  is the donor and  $A$  is the acceptor). The absence of complete charge transfer in the ground state (i.e., the P3OT/ $C_{60}$  system is not ionic) is supported by the fact that the infrared active vibrational modes (IRAV) of P3OT/ $C_{60}$  (5%) are not enhanced in the ground state, whereas in the photoexcited state a significant enhancement is observed due to the increased quantum efficiency for the photogeneration of charged excitations on the polymer chain.<sup>24</sup> In addition, the absorption features characteristic of  $C_{60}^-$  observed at 1.15 and 1.25 eV,<sup>24</sup> and the ESR signal from the  $C_{60}$  anion, are seen only in the photoexcited state, and not in the ground state.<sup>2,4</sup> Finally, the magnitude of the

dark conductivity of P3OT/C<sub>60</sub> (5%) is not consistent with charge-transfer doping in the ground state. In contrast, the photoconductivity is strongly enhanced,<sup>4</sup> indicating that complete electron transfer occurs only in the photoexcited state.

At 1 ps after photoexcitation by a 100-fs pump pulse at 2.01 eV, the PIA spectrum for P3OT/C<sub>60</sub> (1%) consists of a single broad peak at approximately 1.55 eV, Fig. 7(b), with virtually no evidence of the HE and LE features seen in pristine P3OT at 1.9 and 1.2 eV. The risetime of this feature is resolution limited (200 fs). After photoexcitation, the peak shifts to the red, from 1.55 at  $\tau=1$  to 1.45 eV at 100 ps, in contrast to what is observed in MEH- and BCHA-PPV/C<sub>60</sub>. The spectrum at 100 ps closely matches that seen in millisecond PIA experiments,<sup>2</sup> implying that the excited species are essentially identical to those observed in the near steady-state measurements. As previously discussed,<sup>3</sup> the formation of the broad peak at 1.55 eV is characteristic of the charge-separated state, with the electron on the C<sub>60</sub> and the hole on the polymer. Thus the spectra of Fig. 7(b) display the evolution of the initial charge-transfer state to the final charge-transfer state observed in the millisecond time regime. The ultrafast (<1 ps) formation of the charge-transfer band at 1.55 eV demonstrates that the electron transfer occurs on a subpicosecond time scale, confirming earlier estimates based on luminescence quenching.<sup>1</sup>

The dichroic ratio of the HE feature in pristine P3OT (Fig. 8, open circles) in the first picosecond after photoexcitation approaches the theoretical limit of 3, indicating a large contribution from intrachain excitations in this time regime. By 10 ps after photoexcitation the excitations decay and/or diffuse to polymer segments that are randomly oriented with respect to the initial segment, so that the dichroic ratio decreases to 1.6. We attribute this to the polaron exciton, which is short-lived intrachain excitation responsible for the fast component of the PIA dynamics of the HE feature, as discussed above.

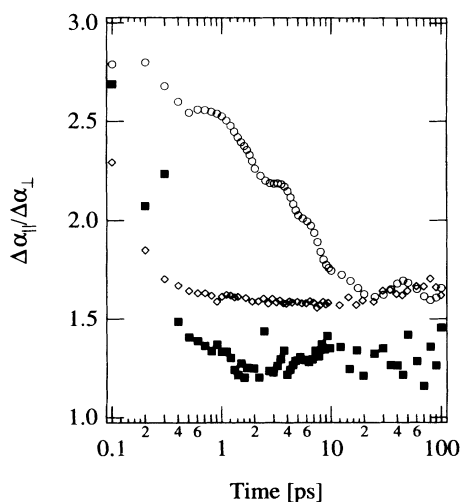


FIG. 8. Dichroic ratio for pristine P3OT at 1.87 eV (open circles), and at 1.21 eV (open diamonds), and for P3OT/C<sub>60</sub> (1%) at 1.5 eV (closed squares), at 300 K.

The dichroism of the LE feature (Fig. 8, open diamonds) begins at 2.25, then drops within several hundred femtoseconds to approximately 1.6, where it remains relatively constant for over 100 ps. The relatively high initial value indicates the importance of intrachain excitations during the first several hundred femtoseconds after photoexcitation. However, the deviation from 3 suggests that interchain excitations might play a role. The electron and hole quickly become separated onto neighboring chains, leading to the rapid decrease in the dichroic ratio to approximately 1.6.

Upon adding 1% C<sub>60</sub> to P3OT (Fig. 8, closed squares), the dichroic ratio at 1.5 eV decreases from 2.7 to 1.5 within 300 fs. The high initial value is again attributed to the initial photogeneration of intrachain excitations on the polymer.<sup>21,25</sup> The dichroism decreases rapidly to 1.5, and then remains relatively constant for over 100 ps. Again, this behavior is attributed to the ultrafast charge transfer. Once the electron transfers to a C<sub>60</sub> molecule, the polarization memory is destroyed. This measurement sets an upper limit of 300 fs on the photoinduced electron transfer time.

In order to compare the time decay of the PIA in pristine P3OT to that of the peak of the PIA feature in P3OT/C<sub>60</sub> (1%), we show the kinetics in P3OT at 1.45 eV (Fig. 9). The fits shown are to the response function  $R(\tau) = Ae^{-t/\tau_1} + Be^{-(t/\tau_2)^{1/3}}$  with  $\tau_1 = 300$  fs and  $\tau_2 = 20$  ps for pristine P3OT (open triangles). The fast component is attributed to the low-energy shoulder of the HE feature, and the slow component is due to the long-lived species that gives rise to the HE and LE bands, as discussed above.

The decay of the photoexcitations in P3OT with 1% C<sub>60</sub> (Fig. 9) fits the same response function used for pristine P3OT. The lifetimes in P3OT/C<sub>60</sub> (1%) are  $\tau_1 = 300$  fs and  $\tau_2 = 25$  ps. The ratio of the coefficients ( $B/A$ ) used

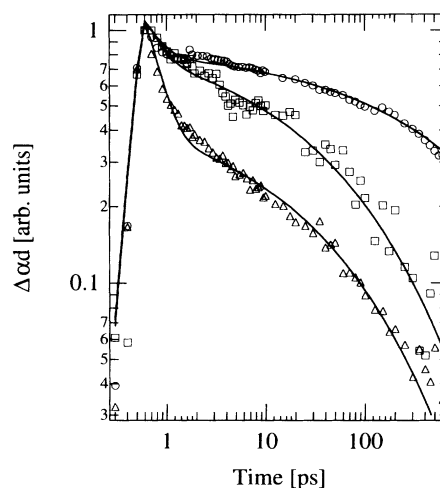


FIG. 9. Decay of the photoinduced absorption at 1.45 eV in pristine P3OT (open triangles), P3OT/C<sub>60</sub> (1%) (open squares), and P3OT/C<sub>60</sub> (10%) (open circles) at 300 K. The fits are to  $R(t) = Ae^{-t/\tau_1} + Be^{-(t/\tau_2)^{1/3}}$ , as described in the text.  $\tau_1$  is 300 fs in each fit,  $\tau_2$  is 20, 25, and 700 ps in pristine P3OT, P3OT/C<sub>60</sub> (1%), and P3OT/C<sub>60</sub> (10%), respectively.



in the fitting increases by over an order of magnitude upon addition of 1%  $C_{60}$ , implying that a much larger fraction of the photoexcitations contribute to the long-lived signal in the composite material than in pristine P3OT. This is consistent with the ultrafast charge transfer, which separates the polaron excitons thereby creating more long-lived charged excitations. The fact that the lifetime of the polaron exciton,  $\tau_1$ , does not decrease due to the faster competing relaxation pathway provided by charge transfer in P3OT/ $C_{60}$  is attributed to the fact that we are nearing the experimental time resolution limit. The lifetime of the stretched exponential,  $\tau_2$ , is increased only slightly from 20 ps in P3OT to 25 ps in P3OT/ $C_{60}$  (1%), implying the kinetics of the long-lived photoexcitations in the 1% composite and in the pristine materials are similar.

The increase in PIA signal in P3OT/ $C_{60}$  (1%) at longer times is attributed to the ultrafast charge transfer which quenches the radiative recombination of the polaron excitons, and increases the yield of photogenerated charged excitations. This conclusion is supported by the dramatic decrease in the quantum yield of luminescence for these materials.<sup>26</sup>

In the P3OT/ $C_{60}$  (10%) mixture, the lifetimes used to fit to the data are  $\tau_1=300$  fs and  $\tau_2=700$  ps. These results are consistent with those obtained earlier using P3OT/ $C_{60}$  (50%)<sup>3</sup> and with photoconductivity measurements<sup>4</sup> made on P3OT/ $C_{60}$  (5%) composites. The increase in  $\tau_2$  observed in the 10% composite implies not only that the charge transfer occurs on a subpicosecond time scale, but also that the back-transfer (i.e., the electron transferring from  $C_{60}^-$  back to P3OT) is inhibited, yielding metastable charge separated photoexcitations.

Each photoexcitation sees roughly ten times more  $C_{60}$  in the 10% composite than in the 1% composite. We find that  $\tau_2$  increases by over an order of magnitude in P3OT with 10%  $C_{60}$  added over the value with 1%  $C_{60}$ , implying the transferred electrons are more deeply trapped in the mixture with the higher concentration of  $C_{60}$ . Assuming that the  $C_{60}$  is homogeneously distributed in the 1% sample, we estimate the minimum average separation between  $C_{60}$  molecules to be on the order of 400 monomer units. The film thickness was measured using a Sloan-Dektak surface profilometer to be roughly  $0.5 \mu\text{m}$ , in which 25% of the pump photons were absorbed. Assuming the density of the P3OT film to be  $1 \text{ g/cm}^3$  yields roughly one photoexcitation every 200 repeat units. Hence the photoexcitation density is of a similar order of magnitude as the  $C_{60}$  density. If the average number of electrons transferred per  $C_{60}$  molecule is greater than one, we may expect that the back-transfer rate may be increased due to Coulomb repulsion between electrons on the  $C_{60}$  dianion. This may explain the small increase in  $\tau_2$  seen in the 1% composite (over that of pristine P3OT). However, if this were the case we would expect  $\tau_2$  to increase as the photoexcitation density decreased, since the probability of transferring more than one electron to a single  $C_{60}$  acceptor would decrease. We found, however, that  $\tau_2$  remained unchanged upon lowering the photoexcitation density by an order of magnitude. This eliminates

multiple electron transfer to a single  $C_{60}$  acceptor as the cause of the shorter lifetime in the 1% composite (compared to the 10% composite).

In P3OT/ $C_{60}$  (10%), the photoexcitation density is much less than the  $C_{60}$  concentration, so that the average electron transferred per  $C_{60}$  molecule is less than one. Viewed through an optical microscope the sample is not homogeneous; some of the  $C_{60}$  has condensed into what appear to be clusters of pure  $C_{60}$ . Hence a large fraction of the photoexcited electrons may transfer not to molecular  $C_{60}$ , as is the case in the 1% composite, but to  $C_{60}$  in the solid state. Since we have established that we are not creating  $C_{60}$  dianions in P3OT/ $C_{60}$  (1%), we conclude that the order of magnitude increase in  $\tau_2$  in the 10% composite results from electrons being more deeply trapped in condensed  $C_{60}$ , possibly due to stabilization of the electron by delocalization over many  $C_{60}$  molecules.

The addition of 1%  $C_{60}$  also affects the dependence of the PIA signal on the incident pump fluence, as shown in Fig. 10. In order to compare with the behavior of the peak of the PIA feature in P3OT/ $C_{60}$ , we consider the intensity dependence of the same spectral region (1.45 eV) in pristine P3OT. At this energy, pristine P3OT follows an  $I^{0.64}$  dependence at 1-ps delay time, which becomes  $I^{0.47}$  by 20 ps. The sublinear dependence seen at early times is attributed to the influence of the polaron exciton. This species is expected to decay geminately and therefore exhibit a linear intensity dependence. However, this dependence is superimposed on the long-lived species which follows a square-root dependence on the pump fluence. This results in an intensity dependence which is intermediate between linear and square root, which persists during the lifetime of the polaron exciton. After the polaron exciton has decayed ( $\tau > 10$  ps) the intensity

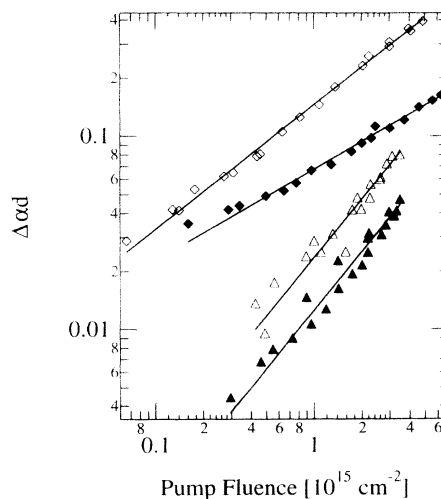


FIG. 10. Dependence of photoinduced absorption on the incident pump fluence for pristine P3OT at 1.42 eV, 1-ps delay time (open diamonds) and at 20-ps delay time (closed diamonds). The same measurement for P3OT/ $C_{60}$  (1%) at 1.42 eV, 1-ps delay time (open triangles) and at 20-ps delay time (closed triangles). The fits are to  $I^{0.64}$  and  $I^{0.47}$  for pristine P3OT at 1 and 20 ps, respectively. Both fits for P3OT/ $C_{60}$  are to  $I^{1.0}$ .



dependence of the entire PIA spectrum follows a square-root behavior. In contrast, the P3OT/C<sub>60</sub> (1%) system displays a linear dependence on pump fluence from the hundred femtosecond time scale to the hundred picosecond time scale. This dramatic difference in the intensity dependence again implies that the electron transfer step dominates the relaxation. The photoexcited electron is transferred within several hundred femtoseconds to a C<sub>60</sub> molecule and upon back transfer to the polymer undergoes monomolecular recombination with a hole on the polymer backbone.

### CONCLUSION

By measuring the dichroic ratio we have demonstrated that photoinduced electron transfer from two PPV derivatives to C<sub>60</sub> occurs within 300 fs of photoexcitation. Due to the separation of the photoexcited electron-hole pair, with electron trapped on C<sub>60</sub>, the lifetime of the photoexcitations are significantly increased in the PPV/C<sub>60</sub> mixtures, with BCHA-PPV/C<sub>60</sub> having the longest lifetime observed in this study. In BCHA-PPV/C<sub>60</sub> the bulky side groups may result in a poor overlap of the excited state wave functions, thereby inhibiting charge transfer of all photoexcited electrons, so that a fraction do not encounter a suitable C<sub>60</sub> acceptor site for several picoseconds. The same mechanism may retard the back transfer, resulting in the long lifetime of photoexcitations seen in this system.

In P3OT/C<sub>60</sub> the time-resolved dichroic ratio again demonstrates that electron transfer occurs within 300 fs of photoexcitation. The rapid, discontinuous decrease in

the dichroic ratio results from spatial separation of electron and hole, with the electron on C<sub>60</sub> and the hole on the polymer backbone. The increase in the quantum efficiency of photogenerated charges is a result of the ultrafast photoinduced electron transfer which quenches the radiative recombination of the singlet polaron exciton by separating the bound electron-hole pair. In the picosecond time scale, at a concentration of 1% by weight of C<sub>60</sub>, this is the dominant mechanism responsible for the increase in the yield of photogenerated charged excitations. Another mechanism that can further increase the lifetime of photogenerated charged excitations is trapping of electrons by C<sub>60</sub>. This yields the slight increase in the lifetime of the charge-separated state on going from pristine P3OT to P3OT/C<sub>60</sub> (1%). The dramatic order of magnitude increase in the lifetime upon going to the 10% composite implies that a high concentration of C<sub>60</sub> results in a deeper trap for the transferred electron. This may be due to aggregation of the C<sub>60</sub> into clusters and stabilization of the transferred electron by delocalization over several C<sub>60</sub> molecules.

### ACKNOWLEDGMENTS

We gratefully acknowledge many useful discussions with Dr. R. Janssen and Dr. K. Pakbaz. This research was supported by the National Science Foundation under Grant No. NSF-DMR90-12808. Funding for the femtosecond laser facility for fast transient spectroscopy was obtained through an NSF Instrumentation Grant No. NSF-DMR90-05866.

\*Present address: Los Alamos National Lab., Los Alamos, NM 87545.

<sup>1</sup>N. S. Sariciftci, L. Smilowitz, A. J. Heeger, and F. Wudl, *Science* **258**, 1474 (1992).

<sup>2</sup>L. Smilowitz, N. S. Sariciftci, R. Wu, C. Gettinger, A. J. Heeger, and F. Wudl, *Phys. Rev. B* **47**, 13 835 (1993).

<sup>3</sup>B. Kraabel, C. H. Lee, D. McBranch, D. Moses, N. S. Sariciftci, and A. J. Heeger, *Chem. Phys. Lett.* **213**, 389 (1993).

<sup>4</sup>C. H. Lee, G. Yu, D. Moses, K. Padbaz, C. Zang, N. S. Sariciftci, A. J. Heeger, and F. Wudl, *Phys. Rev. B* **48**, 15 425 (1993).

<sup>5</sup>N. S. Sariciftci, D. Braun, C. Zhang, V. Srdanov, A. J. Heeger, G. Stucky, and F. Wudl, *Appl. Phys. Lett.* **62**, 585 (1993).

<sup>6</sup>P. M. Allemand, A. Koch, F. Wudl, Y. Rubin, F. Diederich, M. M. Alvarez, S. J. Anz, and R. L. Whetten, *J. Am. Chem. Soc.* **113**, 1050 (1991).

<sup>7</sup>L. Bredas and R. R. Chance, *Conjugated Polymeric Materials: Opportunities in Electronics, Optoelectronics and Molecular Electronics* (Kluwer Academic, Dordrecht, 1990).

<sup>8</sup>W. H. Knox, M. C. Downer, R. L. Fork, and C. V. Shank, *Opt. Lett.* **9**, 552 (1984).

<sup>9</sup>T. F. Albrecht, K. Seibert, and H. Kurz, *Opt. Commun.* **84**, 223 (1991).

<sup>10</sup>M. Sinclair, D. Moses, and A. J. Heeger, *Phys. Rev. B* **36**, 4296 (1987).

<sup>11</sup>T. W. Hagler, K. Pakbaz, K. F. Voss, and A. J. Heeger, *Phys. Rev. B* **44**, 8652 (1991).

<sup>12</sup>L. Smilowitz, N. S. Sariciftci, A. J. Heeger, G. Wang, and J. E. Bowers, *J. Chem. Phys.* **98**, 6504 (1992).

<sup>13</sup>K. Yoshino, H. S. Yin, S. Morita, T. Kawai, and A. A. Zakhidov, *Chem. Express* **7**, 817 (1992).

<sup>14</sup>*Picosecond Electronic Relaxations in Amorphous Semiconductors*, edited by R. R. Alfano (Academic, Orlando, 1984).

<sup>15</sup>C. V. Shank, R. Yen, R. L. Fork, J. Orenstein, and G. L. Baker, *Phys. Rev. Lett.* **49**, 1660 (1982).

<sup>16</sup>S. Takeuchi, M. Yoshizawa, T. Masuda, T. Higashimura, and T. Kobayashi, *IEEE J. Quantum Electron.* **28**, 2508 (1992).

<sup>17</sup>J. L. Bredas and A. J. Heeger, *Chem. Phys. Lett.* **217**, 507 (1994).

<sup>18</sup>N. S. Sariciftci, B. Kraabel, C. H. Lee, K. Pakbaz, and A. J. Heeger, *Phys. Rev. B* **50**, 12 044 (1994).

<sup>19</sup>B. Kraabel, D. McBranch, N. S. Sariciftci, D. Moses, and A. J. Heeger, *Mol. Cryst. Liq. Cryst.* (to be published).

<sup>20</sup>U. Stamm, M. Taiji, M. Yoshizawa, K. Yoshino, and T. Kobayashi, *Mol. Cryst. Liq. Cryst.* **182A**, 147 (1990).

<sup>21</sup>G. S. Kanner, X. Wei, B. C. Hess, L. R. Chen, and Z. V. Vardeny, *Phys. Rev. Lett.* **69**, 538 (1992).

<sup>22</sup>B. Y. Balagurov and V. G. Vaks, *Zk. Eksp. Teor. Fiz.* **65**, 1939 (1973) [*Sov. Phys. JETP* **38**, 968 (1973)].

<sup>23</sup>P. Grassberger and I. Procaccia, *J. Phys. Chem.* **77**, 6281

- (1982).
- <sup>24</sup>K. Lee, R. Janssen, N. S. Sariciftci, and A. J. Heeger, *Phys. Rev.* **49**, 5781 (1994).
- <sup>25</sup>T. Kobayashi, M. Yoshizawa, U. Stamm, M. Taiji, and M. Hasegawa, *J. Opt. Soc. Am. B* **7**, 1558 (1990).
- <sup>26</sup>S. Morita, A. A. Zakhidov, and K. Yoshino, *Solid State Commun.* **82**, 249 (1992).